

MICROSCOPY

Recording the wild lives of immune cells

Mikael J. Pittet^{1,2*}, Christopher S. Garriss^{1,3}, Sean P. Arlauckas^{1,2}, Ralph Weissleder^{1,2,4}

Intravital microscopic imaging can uncover fundamental aspects of immune cell behavior in real time in both healthy and pathological states. Here, we discuss approaches for single-cell imaging of adaptive and innate immune cells to explore how they migrate, communicate, and mediate regulatory or effector functions in various tissues throughout the body. We further review how intravital single-cell imaging can be used to study drug effects on immune cells.

INTRODUCTION

We are at a point in immunology at which we appreciate the complexity of the relationships between immune cell populations and disease states. Unraveling this complexity requires a palette of research tools with which to investigate immune cell subpopulations and their functions. Selecting the proper tools for a specific application and model requires knowledge of each technology's strengths and limitations. The immunology field has historically focused on classifying immune cells by first isolating and then studying them by using multiplexed cytometry. More recently, the introduction of single-cell transcriptomics has given us the ability to collect unbiased information on all cell populations. In contrast to these *ex vivo* approaches, intravital imaging enables direct visualization of immune cells and their functions in various tissues *in vivo*, without the need for isolation and selection procedures that can introduce bias. Intravital imaging is particularly suited to dynamically visualize immune cells over time, often revealing previously unknown behaviors. Many immune functions are heavily dependent on cell migration and cell-cell contacts, both of which can be faithfully captured with single-cell resolution intravital imaging. Spatial organization can dictate the effective functionality of immune cells, which is readily apparent from imaging studies but may not be detected by using traditional cell profiling methods. Furthermore, the ability to quantitatively measure kinetics of behaviors provides key insights into immune processes and even potentiates mathematical modeling of emergent behaviors. Here, we focus on how immunologists can use intravital single-cell imaging approaches to complement superresolution imaging in isolated cells (1) and imaging at the whole-body level (2).

THE TOOLBOX

A number of intravital imaging approaches exist, and their basics and general implementations have been covered already (3–5). This section therefore focuses on specifically adapting these technologies to observe how immune cells travel, function, and interact in live mice.

What are the different intravital imaging approaches available, and what are their advantages and limitations?

Today's two main approaches for single-cell imaging use either confocal laser scanning or multiphoton microscopy. The systems are

¹Center for Systems Biology, Massachusetts General Hospital, 185 Cambridge Street, CPZN 5206, Boston, MA 02114, USA. ²Department of Radiology, Massachusetts General Hospital, Boston, MA 02114, USA. ³Graduate Program in Immunology, Harvard Medical School, Boston, MA 02115, USA. ⁴Department of Systems Biology, Harvard Medical School, 200 Longwood Avenue, Boston, MA 02115, USA.

*Corresponding author. Email: mpittet@mgh.harvard.edu

generally implemented on upright microscopes, and several configurations are now commercially available. Most intravital imaging setups for mice now have an upright configuration, although in some cases, inverted systems are also used. The latter may be beneficial for dual-purpose cell and tissue imaging systems or for exteriorized organs that assume a flat configuration on the glass. Confocal microscopy setups are usually less expensive and represent a good all-around technique for much of the imaging performed today (6). These systems use an array of solid-state lasers for excitation, and matched laser and filter sets can demultiplex fluorophore signals, similar to flow cytometry. The down sides of confocal imaging are higher autofluorescence and scattering, which generally limit imaging depths to <100 μm and typically in the range of 20 to 50 μm . Furthermore, shorter-wavelength channels have higher phototoxicity, although this is often a lesser concern for *in vivo* imaging than it is for *in vitro* imaging.

Multiphoton laser scanning microscopy (7) bypasses the limitations of confocal microscopy by using more expensive and tunable titanium:sapphire lasers that operate in the near-infrared range. Localized nonlinear excitation based on two-photon absorption allows for superior tissue penetration at higher wavelengths and less out-of-focus excitation. One of the major ways in which multiphoton imaging reduces phototoxicity and improves resolution is through inherent optical sectioning because of the more restricted photon excitation volume. Typical penetration depths are in the range of 200 to 300 μm for most organs, except in the brain and cleared tissues, where deeper imaging depths can be achieved. Multiphoton microscopy can induce photobleaching, but again, this is often less of a concern for *in vivo* imaging. One minor disadvantage of the multiphoton system is that many of the fluorophores used in flow cytometry, epifluorescence, and confocal microscopy experiments have not been characterized in the multiphoton setup.

What are the key requirements for a single-cell imaging experiment?

To perform state-of-the-art single-cell three-dimensional (3D) imaging, one requires (i) an integrated imaging system in a dark and appropriately cooled room [(4), supplementary materials], (ii) suitable fluorescent reporter mouse models with either exteriorized organs (8) or implanted window chambers (9), (iii) motion suppression techniques (10), (iv) physiologic support modules, and (v) data processing and analytical software (Fig. 1). Physiologic support, including feedback temperature controls, is critical to maintaining homeostasis and hydration in immobilized and ventilated animals. This support is most commonly achieved by using warming plates, immobilization chambers, and continuous vital sign monitoring while the animal is anesthetized. Temperature control in exteriorized organs is especially critical to preserve cell motility.

Copyright © 2018
The Authors, some
rights reserved;
exclusive licensee
American Association
for the Advancement
of Science. No claim
to original U.S.
Government Works

Quality control measurements include calibrating the imaging system with fluorescent bead phantoms, correcting artifacts, detecting channel bleed-through, determining the stability of reporter expression levels, and properly managing data outliers. Data processing and analysis is a major part of a single-cell imaging experiment. Various software packages automate the analysis of high-dimensional data, although manual curation is still often necessary. Common software packages that support image processing, segmentation, cell measurements, and profiling features include CellProfiler, Fiji, Imaris, and microscope vendor packages. MATLAB and Python are programming languages that are also used to implement postprocessing algorithms and quantitative analysis, whereas widely available pack-

ages such as GraphPad Prism or CellProfilerAnalyst are used for statistical analyses of extracted features across study groups, findings, and data sets.

Common approaches

Before performing an imaging experiment, the questions to be answered should be clearly outlined, and all experimental variables should be considered. What type of information can be retrieved, and how many parameters can be measured simultaneously? The answers to these questions will vary from organ to organ, but it is generally accepted that up to four (confocal) or six channels (multiphoton) can be acquired during a typical 3D acquisition. Most often, these channels are

reserved for different immune cell populations (11), structural content (collagen fibers or vessels), or labeled drugs (12). Inhalation-anesthetized mice bearing window chambers generally tolerate repeat imaging well and can be effectively analyzed on subsequent days, unless non-survival surgery is performed on exteriorized organ preparations; in such a case, it is important to maintain the homeostatic environment with respect to blood flow and oxygen supply in addition to temperature. The typical imaging session varies in length but often lasts 1 to 2 hours unless slower phenomena are being studied. The most commonly imaged organ systems are tumors, lymph nodes, and the skin but also include brain, bone marrow, kidney, liver, lungs, pancreas, reproductive tract, spleen, and yolk sac (Fig. 2, A and B).

Window chamber models (9, 13) are particularly suited for intravital imaging because they can be easily accessed and immobilized. They also offer the possibility to investigate a wide range of pathological conditions, including autoimmunity (14), infection (15), and cancer (16). The installation of these immobilizing devices requires administration of a postoperative analgesic, which is often butenorphine. Antibiotics or antimycotics can also be given to mitigate the risk of infection at the surgical site. Additional considerations may be taken concerning the housing and handling of the mice so as to avoid damaging the chamber if the animal is to be monitored over repeated imaging sessions. Typically, imaging is initiated several days after the chamber is implanted, when surgery-induced inflammation has resolved. However, it is always critical to assess whether the procedure used to prepare the mouse affects the readouts to be recorded during the imaging session; this should be performed, at least in part, by imaging mice that underwent

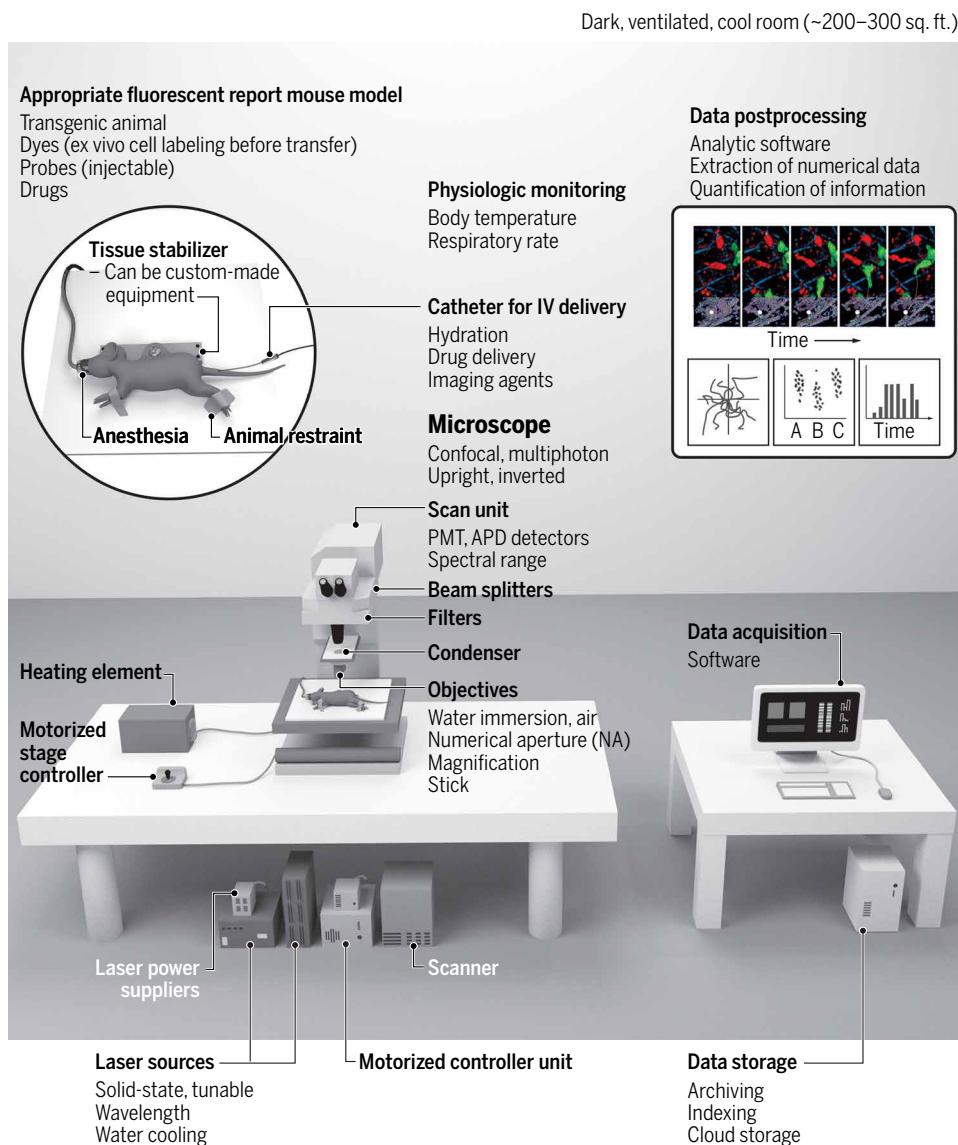


Fig. 1. Diagram of an intravital imaging setup. (Left) The equipment required for conducting an intravital imaging experiment includes an appropriate fluorescent mouse model, a microscope (shown here is an upright multiphoton microscope), laser sources, physiological monitoring, an appropriate anesthesia setup, and a tissue stabilizer to prevent motion artifacts during imaging. This image illustrates imaging in a dorsal skinfold window chamber; other tissues can be imaged (Fig. 2), each of them requiring their own methods of tissue preparation, stabilization, and monitoring. PMT, photomultiplier tube; APD, avalanche photodiode. (Right) Data acquisition, followed by data storage and data postprocessing to extract quantitative information.

sham surgery. Detailed methods are available for intravital imaging of various organs such as lymph nodes (17), tumors (13, 18, 19), ear skin (20), abdominal tissues (21–23), lung (9), and heart (24).

INTRAVITAL IMAGING TO STUDY ADAPTIVE IMMUNITY

Cell migration and cell-cell interactions play pivotal roles in adaptive immunity. For instance, circulating naive T cells continuously home to secondary lymphoid organs, where they physically engage with antigen-presenting cells. Local encounters with cognate antigen can produce activated T cell progeny, including effector, central, and tissue-resident memory subsets, which gain distinct migratory and functional abilities. Cells that traffic to sites of inflammation can further interact with antigen-bearing and other cells and mediate effector functions. Single-cell imaging enables the direct study of

all these dynamic processes in complex microenvironments and various tissues.

T cells

The least invasive methods to image T cells use genetic mouse models in which endogenous T cells selectively express a fluorescent protein reporter (Table 1). This approach can assess T cell infiltration in various tissues (11, 25) and bypasses ex vivo cell manipulation and transfer, which may affect cell behavior and fate. Endogenous T cells may behave differently from adoptively transferred ones. Ideally, one would want to image endogenous T cells by using mouse models that have T cell-specific reporters, whereas adoptive transfer should be considered in special cases. Genetic mouse models can also be used for tracking regulatory T (T_{reg}) cells, which has been performed in lymph nodes (26), bone marrow (27), and nonlymphoid tissues (28).

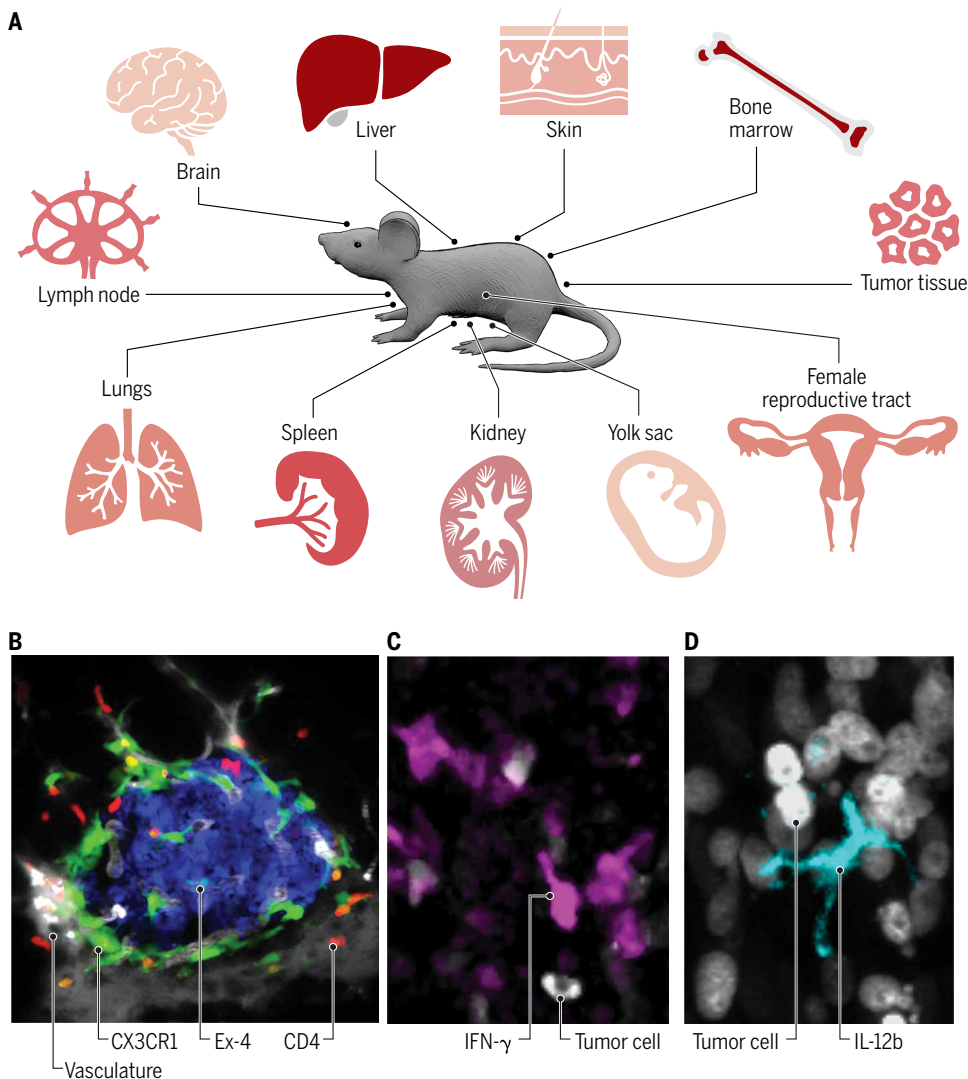


Fig. 2. Existing applications of immune cell imaging in various tissues. (A) A wide range of mouse tissue sites is adapted for single-cell imaging. (B) Intravital micrograph showcasing detection of two immune cell types, namely, $CD4^+$ T cells (red) and $CX3CR1^+$ macrophages (green) in pancreatic islets. β cells (blue) were visualized with exendin-4 (Ex-4)-like neopeptide conjugated to the fluorescent dye Se-Tau-647, and the vasculature was detected with 500 k molecular weight dextran conjugated to a Pacific blue dye (gray). (C and D) Intravital micrographs showcasing detection of cytokines produced by immune cells in live mice, here in tumor tissues. (C) $IFN-\gamma$ -producing lymphocytes (magenta). (D) $IL-12b$ -producing myeloid cells (cyan). Tumor cells are also shown (gray).

CREDIT: A. KITTERMAN/AAAS

However, in practice, intravital T cell tracking still often relies on adoptive cell transfer approaches. Here, T cells of interest are first purified from mice ubiquitously expressing a fluorescent protein reporter and then administered into recipient mice, so transferred cells and their progeny can be visualized within a tissue of interest (Table 1). This approach is convenient because it allows one to control the quantity of visible (exogenously added) cells in a given field of view. By contrast, the density of endogenous T cells in tissues such as lymph nodes is often quite high, making it difficult to distinguish individual cells.

Intravital imaging of adoptively transferred T cells has uncovered how naive (29, 30) and central memory (31, 32) T cells sense antigens and become activated in lymph nodes. For instance, imaging has revealed that naive lymph node $CD8^+$ T cells are initially motile, which allows them to undergo multiple transient contacts with antigen-presenting dendritic cells (DCs), but can then progressively decrease their motility to form stable contacts with DCs, at which time, they also start producing effector cytokines. The T cells eventually resume their migration, begin to proliferate, and can emigrate from the lymph node (29). The type of interaction that a $CD8^+$ T cell undergoes with an antigen-presenting DC depends, at least in part, on the antigen dose. Whereas low-antigen-dose conditions can functionally prime $CD8^+$ T cells, only a high antigen dose may trigger stable T cell–DC contacts (8); these longer contacts may be necessary for the generation of full-fledged immune responses. Intravital lymph node imaging has further revealed that helper $CD4^+$ and $CD8^+$ T cells are largely compartmentalized

Table 1. Reporter systems to track different immune cells and their functions by single-cell imaging. This list serves as a general survey of intravital imaging labeling strategies across cell types; however, numerous Cre strains can additionally be incorporated into useable reporter systems. CFP, cyan fluorescent protein; DsRed, *Discosoma* sp. red fluorescent protein; FOXP3, forkhead box P3; TBX21, T-box 21; eGFP, enhanced GFP; Bcl6, B cell lymphoma 6; pDCs, plasmacytoid DCs; Zbtb46, zinc finger and BTB domain containing 46; Csf-1, colony-stimulating factor 1; AID, activation-induced cytidine deaminase; DTR, diphtheria toxin receptor.

| Reporter | Notes | Examples |
|---|---|----------|
| <i>T cells</i> | | |
| GFP, CFP, DsRed | Requires adoptive cell transfer | (29) |
| PA-GFP | Photoactivatable fluorescent reporter useful for cell tracking; requires adoptive cell transfer | (51) |
| DPE -GFP | A pan T cell marker; can also label pDCs | (25) |
| NFAT-GFP, NFAT-YFP;H2B-mCherry | Readout of TCR signaling | (43) |
| IFN- γ -YFP | Subset of activated T cells; can also be produced by NK cells | (25) |
| IL-10-GFP | Subset of T cells; can also be expressed by macrophages | (43) |
| FOXP3-GFP, FOXP3-mRFP | Labels T _{reg} cells; FOXP3 is on the X chromosome, be aware of X chromosome inactivation in females | (27) |
| Nur77-GFP | Labels T cells and also B cells upon antigen receptor engagement | (110) |
| Granzyme B-TdTomato | A marker of granule exocytosis in cytolytic T cells and NK cells | (111) |
| Tbx21-ZsGreen | For assessing T _H 1 responses in T cells | (112) |
| CD2-eGFP | Labels peripheral T cells and some NK subsets | (113) |
| IL-17F-Cre ^{eYFP} | Many variants exist for studying T _H 17 cells in vivo | (114) |
| IL-4-eGFP | Used to assess T _H 2 immunity | (115) |
| IL-21-GFP | Used to study the role of T _{FH} cells | (116) |
| <i>B cells</i> | | |
| GFP, CFP, DsRed | Requires adoptive cell transfer | (117) |
| PA-GFP | Photoactivatable fluorescent reporter useful for cell tracking; requires adoptive cell transfer | (51) |
| CD19-tdRFP | Expressed by numerous B cells, adoptive transfer may be necessary if tissues are densely infiltrated by B cells | (49) |
| Bcl6-YFP | A B cell marker already validated for two-photon microscopy; also labels T _{FH} cells | (118) |
| Blimp-1-YFP | Expressed by B cells and highly expressed in plasma cells | (119) |
| Activation-induced cytidine deaminase (AID)-GFP | Subset of B cells | (120) |
| <i>DCs</i> | | |
| CD11c(ITGAX)-YFP, CD11c-mCherry | Cells other than DCs can express CD11c | (121) |
| XCR1-Venus/+ | Homozygous mice are null for XCR1 | (55) |
| XCR1-KIKGR/+ | Xcr1 replaced with photoconvertible fluorescent protein Kikume Green-Red (KikGR) | (55) |
| CXCL9-RFP, CXCL10-BFP | These chemokines can also be expressed by other cell types, including monocytes, macrophages, granulocytes, and nonimmune cells | (32) |
| SIGLEC-H-GFP | Expressed by pDCs | (54) |
| Flt3-BFP2 | This construct has also been incorporated into a genetic model used to visualize DCs, macrophages, and CD4 ⁺ and CD8 ⁺ T cells simultaneously (Flt3-BFP2, Mertk-GFP-diphtheria toxin receptor, Cd4-tdTomato, Cd8a-tdTomato) | (11) |
| Zbtb46-GFP | A cDC marker that may be expressed in erythroid and endothelial populations | (122) |
| <i>Monocytes/macrophages</i> | | |
| CX3CR1-GFP/+ | This chemokine receptor can also be expressed by T cells, NK, DC, and macrophages. Homozygous mice are null for CX3CR1 | (123) |
| CCR2-RFP/+ | Homozygous mice are null for CCR2 | (61) |
| CX3CR1-GFP/+;CCR2-RFP/+ | Homozygous mice are null for CX3CR1 and/or CCR2 | (61) |
| Mertk-GFP-DTR | Homozygous mice are null for MerTK | (11) |

continued on next page

| Reporter | Notes | Examples |
|---|--|----------|
| c-fms-GFP | c-fms is also known as Csf-1 receptor | (60) |
| MacBlue | A gal4-responsive UAS-ECFP cassette also under the Csf-1 receptor promoter | (124) |
| Dye-conjugated ferumoxytol | Administered to mice several hours before imaging | (25) |
| Dye-conjugated dextrans and dextran nanoparticles | Administered to mice several hours before imaging; can be used to label blood vessels in short term after administration | (71) |
| Dye-conjugated anti-CD169 mAb | Used to label SCS macrophages | (125) |
| Dye-conjugated anti-F4/80 mAb | A pan macrophage marker in mice | (61) |
| <i>Neutrophils</i> | | |
| Dye-conjugated anti-Ly-6G mAb | Imaging is performed shortly after administration (~15 min) | (126) |
| Dye-conjugated anti-Gr-1 mAb | Imaging is performed shortly after administration (~15 min) | (126) |
| LysM-GFP | Can also be expressed by macrophages | (77) |
| Dye-conjugated anti-neutrophil elastase mAb | Imaging is performed shortly after administration (~15 min) | (85) |
| CXCL12-mRFP | Can also be expressed by stromal cells | (80) |
| SYTOX Green | Used to visualize NETs (extracellular DNA labeling); also demarcates cell death | (85) |
| <i>Innate lymphocytes</i> | | |
| GFP, CFP, DsRed | Requires adoptive cell transfer | (92) |
| CXCR6-GFP | Can be used to track ILCs and iNKT cells but is also expressed by some T cells | (89) |
| <i>Megakaryocytes and platelets</i> | | |
| PF4-cre tdTomato | Labels megakaryocytes as well as platelets, which are defined based on their smaller size | (88) |
| Dye-conjugated anti-CD49b mAb | Labels all platelets | (85) |
| CD41-YFP ^{ki/+} | Labels a fraction of platelets | (85) |
| <i>HSC-derived cells</i> | | |
| GFP, CFP, DsRed | Requires adoptive cell transfer and is used to track HSCs and their progeny | (84) |
| <i>Nonimmune components</i> | | |
| Dye-conjugated anti-Lyve-1 mAb | Labels lymphatics | (45) |
| AngioSPARK | Labels blood vessels | (71) |
| Second-harmonic generation | Applicable to multiphoton (not confocal) microscopy; enables visualization of collagen fibers | (91) |
| IL-7-eCFP | Expressed by stromal cells in thymus and bone marrow | (44) |
| GCaMP6s | Sensor of calcium flux; relevant in the context of, for example, virus-infected cells | (39) |
| qDots | Bright, highly tunable fluorophores surface-engineered to maximize circulation | (127) |
| Isolectin | Used to label endothelial wall of blood vessels | (128) |
| Hoechst33342 and CellTracker dyes | Indiscriminately labels cell nuclei or cytosol; often used for adoptive cell transfer | (41) |

during priming reactions; however, during later phases of lymphocyte maturation, these cells are brought together by some DCs. This process enables the delivery of CD4⁺ T cell help to CD8⁺ T cell responses, which is important for the generation of CD8⁺ T cell memory (30).

Intravital imaging in the context of vaccinia virus infection has further revealed the compartmentalization of naive and memory CD8⁺ T cells in lymph nodes. Whereas naive CD8⁺ T cells primarily locate in the cortex, memory CD8⁺ T cells distribute along the periphery of the lymph node (33). This distinction is likely relevant because it brings memory CD8⁺ T cells in close proximity to subcapsular sinus (SCS) macrophages, which are among the first lymph node cells to capture lymph-borne viruses. Therefore, it appears that memory CD8⁺ T cells have preferential access to antigen upon viral reinfection (31, 33). Other imaging studies have tracked T cells in

nonlymphoid tissues. For example, skin and female reproductive tract imaging have defined antigen-specific resident memory T cell (T_{RM}) activation and proliferation in response to viral infections (34, 35). T_{RM} responses in the female reproductive tract can occur in the absence of DCs (35); however, it is unknown whether T_{RM} responses in other tissues require these cells.

Additional imaging tools extend our ability to study T cell communication with neighboring cells at a deeper level so that specific molecular outcomes can be identified (Table 1). For example, transgenic mice harboring a T cell receptor (TCR)-green fluorescent protein (GFP) fusion protein enable the visualization of TCR clustering and internalization after antigen encounter (36). Translocating nuclear factor of activated T cells (NFAT) from the cytoplasm to the nucleus is a sensitive readout of TCR signaling and can be assessed with intravital

imaging by use of fluorescently labeled NFAT (37). The NFAT reporter is often used in combination with fluorescently labeled histone protein histone 2B (H2B), a nuclear marker. Other cell signaling mechanisms such as calcium flux can be detected by using transgenic mice that express the calcium sensor protein GCaMP6s to read out features such as *in vivo* T cell activation (38) or target cell killing (39).

CD8⁺ T cells can also be caught in the act of effector activities. For instance, intravital imaging approaches have shown blood circulating CD8⁺ T effector cells to adhere onto liver sinusoids and engage in immune surveillance (40) and cytotoxic T cells to kill virus-infected cells in lymph nodes (39). The latter study used color-labeled viruses to visualize virus-infected cells and identified that T cell-mediated target cell killing *in vivo* may be much slower than anticipated from previous *in vitro* studies. Interestingly, the proximity of T_{reg} cells can dramatically slow the kinetics of CD8⁺ T cell killing *in vivo* (41). Cytokines such as interferon- γ (IFN- γ) and interleukin-10 (IL-10), both produced by T cells, can also be detected with intravital imaging. Because IFN- γ has a rapid on/off cycling (42), a common readout typically requires restimulation of T cells *in vitro* with an antigenic trigger. This method is useful to define whether given cells are equipped to produce

IFN- γ , but it cannot assess whether these cells actually produced the cytokine *in vivo*. By contrast, intravital imaging of IFN- γ -internal ribosome entry site–yellow fluorescent protein (IFN- γ -IRES-YFP) reporter mice detects YFP, which is expressed by cells that have turned on IFN- γ production (25). YFP remains detectable even after IFN- γ production is turned off, which makes intravital imaging a particularly useful tool with which to detect IFN- γ pathway activation *in vivo* (Fig. 2C), although it cannot identify cells that are currently producing the cytokine. Imaging is also useful to detect cells that produce IL-10, which was identified as a factor important for both viral containment and tissue protection after vaccinia virus infection (43). IL-7—which is required for T cell development, survival, and memory development—can also be tracked in IL-7 reporter mice. Imaging of IL-7 reporter systems has provided useful information of the location and composition of IL-7-dependent immune cell niches (44).

B cells

Intravital B cell tracking, such as T cell tracking, usually involves transgenic reporter mice or adoptively transferring fluorescent B cells into recipient mice (Table 1). Both approaches enable the study of

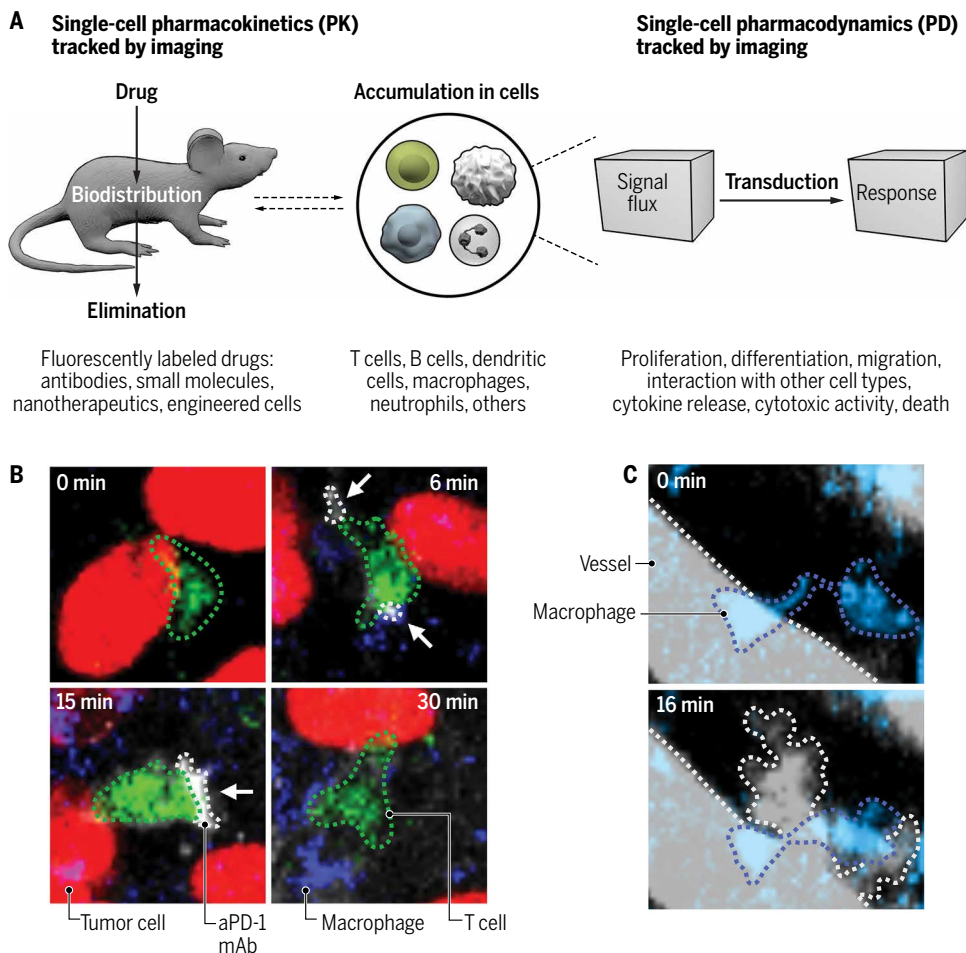


Fig. 3. Single-cell imaging of drugs and their effects on immune cells. (A) Intravital imaging can reveal drugs' (left) PK and (right) PD at single-cell resolution. The examples listed below indicate which types of drugs, cells, and responses can be detected and are relevant to immunology. (B) A PK study reveals that the immune checkpoint blocker anti-PD-1 mAb (aPD-1 mAb; gray) binds to T cells (green) only transiently in the tumor stroma (25). (C) A PD study reveals that radiation therapy primes tumor-associated macrophages (blue) to initiate vascular bursts. (With the permission of M. Miller, Massachusetts General Hospital, Boston.)

B cells in different body compartments. In lymph nodes, intravital imaging has shed light into how B cells interact with various cellular and molecular components—including SCS macrophages (45), T follicular helper (T_{FH}) cells (46), and type I IFN (38, 47)—and how these dynamic interactions regulate the initiation of humoral immune responses. For example, in the context of infection, intravital imaging studies have revealed that lymph-borne viruses preferentially infect SCS macrophages, which then present viral particles to B cells to initiate humoral immune responses (45). Intravital imaging studies further identified that B cells can express intercellular adhesion molecule 1 (ICAM1) and ICAM2, which are critical for forming stable contacts between B cells and T_{FH} cells and subsequent development of humoral immunity (46). By contrast, imaging studies have shown that type I IFN inhibits antiviral B cell responses in lymph nodes—for example, by recruiting inflammatory monocytes that produce nitric oxide (47) and by activating cytotoxic T lymphocytes that kill antiviral B cells (38). Not all T cell–B cell interactions in lymph nodes stimulate humoral immunity; cytotoxic T lymphocytes can kill B cells under certain contexts (38, 41).

Intravital imaging has been further used to study B cells in other tissues. For example, intravital imaging revealed how splenic B cells shuttle antigens from the marginal zone and into B cell follicles (48). B cell imaging has also been extended to various bone compartments by using novel

imaging platforms that allow for long-term, longitudinal studies of bone marrow dynamics (49) and to nonlymphoid tissues such as the lungs and liver (50). For example, pulmonary intravital imaging has revealed that B cells can physically interact with aged neutrophils and contribute to their clearance locally (50).

By transferring B cells that carry the photoactivatable GFP (PA-GFP) reporter, it is possible to tag these cells through multiphoton photoactivation within distinct microanatomical tissues such as the germinal center of a lymph node (51). This photoactivation system in situ was used to interrogate migratory behavior of B cells within germinal centers and identify that cell proliferation occurs in the dark zone of the germinal center after B cells are instructed by T cells in the light zone of the germinal center (51). The photoactivated cells can be monitored in vivo for up to several days or purified for additional analysis in vitro. In principle, this approach can be used to tag any adoptively transferred cell, regardless of its type, and be further extended to photoconvertible fluorescent reporters, such as Kaede and Dendra2, which shift from green to red fluorescence upon exposure to light of appropriate wavelength (4). These types of experiments enable investigators to have finer spatial resolution of migratory phenotypes because photoconversion of cells can identify distinct migratory properties that would otherwise be difficult to study. In addition, photoactivation models can be used in combination with single-cell sequencing approaches to retain spatial information in high-dimensional sequencing technologies (52).

INTRAVITAL IMAGING TO STUDY INNATE IMMUNITY

An increasing number of tools are available to image a variety of innate immune cell types, including DCs, monocytes, macrophages, neutrophils, and innate lymphocytes. Single-cell imaging is most often used to understand innate immune cells' interplay with their adaptive counterparts or to reveal their functions in development, steady state, health, and disease.

Dendritic cells

Both genetic reporter and adoptively transferred DCs can be tracked with intravital imaging (Table 1). *CD11c*-YFP reporter mice have been used to yield insight into how endogenous DCs are spatially organized in lymph nodes, collect antigens, and promote T cell responses to these antigens (30, 53). However, other cell types including macrophages may express CD11c. Endogenous DCs can also be imaged by using *Flt3*-BFP2 (11) or *XCR1*-Venus (54) reporter systems. Typically, all DC subsets express *Flt3* (fms-like tyrosine kinase 3), whereas macrophages and other cells usually do not or do so at much lower levels. *XCR1* (X-C motif chemokine receptor 1) expression is more selective for a subtype of DCs, whereas CD11c is expressed by DCs but also by some macrophages and T cells. An *XCR1*^{KiGRV+} genetic mouse model further enables photoconversion of *XCR1*⁺ DCs in vivo (55). These mice are convenient for tracking migratory DCs and distinguishing them from neighboring resident DCs. For instance, skin *XCR1*⁺ DCs photoconverted by means of violet-blue illumination can be tracked upon migration to skin-draining lymph nodes and discriminated from nonphotoconverted DCs (55). This approach identified that skin *XCR1*⁺ DCs that migrate to draining lymph nodes gradually accumulate in deep medullary regions of the T cell zone, where they can prime naive CD8⁺ T cells (55). Painting the skin with a fluorescent dye, such as tetramethyl rhodamine isothiocyanate (TRITC), may also distinguish recent skin DC migrants,

which carry the dye, from other lymph node DCs (56), although it is formally possible that some dyes may percolate to lymph nodes independently of DCs or be transferred from one cell type to another. In the context of herpes simplex virus type 1 infection, TRITC-labeled DCs accumulate in the T cell zone of draining lymph nodes, where they interact predominantly with naive CD4⁺ but not CD8⁺ T cells. CD8⁺ T cell activation occurs about 1 day later and involves *XCR1*⁺ (TRITC⁻) DCs, suggesting that distinct DC subsets activate CD4⁺ and CD8⁺ T cells sequentially. Eventually, clusters of *XCR1*⁺ DCs and activated CD8⁺ T cells recruit the preactivated helper CD4⁺ T cells, which provide licensing signals to enhance CD8⁺ T immunity (56). The formation of a ménage-à-trois between DCs and CD4⁺ and CD8⁺ T cells can also be promoted by clusters of DCs and CD4⁺ T cells that recruit naive CD8⁺ T cells (57).

Some DC functions can also be imaged. For example, a transgenic mouse reporting expression of the chemokines CXCL9 and CXCL10 (which bind the chemokine receptor CXCR3, expressed by T cells) has demonstrated that DC-derived CXCL10 facilitates interactions between DCs and naive CD4⁺ T cells in the T cell zone. Both CXCL10 and CXCL9 (produced by stromal cells) further guide activated CD4⁺ T cells away from the T cell zone and into interfollicular and medullary zones of the lymph node. This process is important for the development of the T helper 1 (T_H1) subtype of CD4⁺ T cells, presumably because it enables CD4⁺ T cells to receive stimuli from cell populations located in the periphery of the lymph node, including SCS macrophages (7, 32). Cytokines such as IL-12, which can be produced by DCs to activate T cells, are also detectable with intravital imaging (Fig. 2D).

Monocytes and macrophages

Intravital imaging has been used to examine macrophages in various tissues, including lymph nodes (58), tumors (25, 59, 60), liver (61), lung (62), pancreas (11), kidney (63), and the brain (64). Macrophages can be viewed by using genetic reporters such as MerTK (Mer tyrosine kinase)-GFP (11) or after in vivo labeling with fluorescent nanomaterials (Table 1) (65). Furthermore, imaging has been used to study several macrophage immune functions, including microenvironmental surveillance (66), bacteria capture (67), adaptive immune response stimulation (58), extracellular matrix remodeling (68), and tissue repair (61), as well as perhaps less expected functions such as shielding injured cells (69), exchanging cytoplasm with neighboring cells (70), and promoting vasculature bursting (71).

Macrophages that accumulate in inflammatory sites typically originate from circulating monocytes, which can be detected by using CX3CR1 reporter mice (72). The same mice can be used to track splenic reservoir monocytes and their deployment to the circulation in response to inflammatory cues (73). In addition, CX3CR1-GFP;CCR2-RFP (red fluorescent protein) mice can be used to distinguish between monocyte/macrophage subsets that express these chemokine receptors at different levels (61). These mice were used to show that mature macrophages from the peritoneal cavity can migrate to the liver after acute injury (61), challenging the paradigm that macrophages are sessile immune cells. In contrast to macrophages in inflammatory sites, many macrophages found in resting adult tissue are established before birth. Imaging can also be used to track the development of the immune system through embryonic precursor populations by using CX3CR1 reporter models. These approaches have shown how yolk sac premacrophages migrate to the developing embryo and seed macrophage pools (74).

Neutrophils

Neutrophils have been imaged in various tissues such as liver (75), lung (76), skin (77), spleen (78), joints (79), trachea (80), and tumors (81). Methods to track neutrophils rely either on tagging them with fluorescent antibodies, such as anti-Ly-6G monoclonal antibodies (mAbs), or using genetically encoded reporters, such as LysM (M lysozyme)-GFP (Table 1). The antibodies used to tag neutrophils are given at lower doses than for cell depletion studies, and the neutrophils are imaged shortly (~15 min) after intravenous mAb administration. Such approaches require testing that the injected mAbs label the targeted cells without substantially altering their fate. In addition, care must be taken in interpreting LysM-GFP studies because macrophages can also express LysM. Neutrophil extracellular traps (NETs), which are composed of DNA and are released by neutrophils to eliminate extracellular pathogens, can be visualized by using nucleic acid-labeling agents (such as SYTOX Green) or antibodies against extracellular histones or neutrophil elastase (82). In sterile liver injury models, photoactivatable cell-tracking approaches have started to reconstruct the journey of neutrophils. These studies identified that neutrophils, initially produced in the bone marrow, are recruited to the injury site, where they mediate key effector functions, then reenter the circulation, and relocate to the lung and eventually the bone marrow, where they are eliminated (75). The implications for neutrophil egress from injury sites, and homing back to the sites where they were produced, require further study.

Other hematopoietic cells

Hematopoietic stem cells (HSCs), megakaryocytes, platelets, eosinophils, and innate lymphocytes can also be tracked in living animals (Table 1). For example, intravital imaging of the mouse calvarium has helped characterize the location and composition of HSC niches in the bone marrow (27, 83). HSC progeny can also be tracked in extramedullary tissues (84). In addition, CD41-YFP and Pf4-cre:mTmG transgenic mice are useful for detecting megakaryocytes and the platelets they produce. Intravital imaging studies have revealed platelets' contributions to host defense. For example, they can promote the release of NETs to protect host cells from virus infection (85), collaborate with Kupffer cells to encase bacteria (86), help circulating T cells to probe for the presence of antigens (40), and migrate at sites of vascular injury to collect bacteria (87). Intravital imaging also identified the lung as an unexpected site of platelet production (88). Imaging has also been used to track eosinophils within mouse airways (84). Last, imaging studies have started to assess innate lymphocytes in various settings such as tissue repair (89), stroke (90), skin homeostasis (91), tumors (92), and patterning immune responses in lymph nodes (33, 93). Innate lymphocyte imaging largely relies on CXCR6 reporter mice; invariant natural killer T cells (iNKT cells) and type 2 innate lymphoid (ILC2) cells express this chemokine receptor, although other cell types may as well.

INTRAVITAL IMAGING TO STUDY DRUGS AND THEIR EFFECTS ON IMMUNE CELLS

A major development in single-cell imaging has been the ability to track drugs in complex tissue microenvironments (12). When combined with immune cell reporters, single-cell imaging can uncover pharmacokinetics (PK) and pharmacodynamics (PD) at the single-cell level with unparalleled insight into drug resistance (25) and mechanism of action (Fig. 3A) (94). For PK studies, fluorescently

labeled drugs are imaged over time to follow their distribution and cell tropism. The approach requires validation that the fluorescent drug retains biological activity, which appears to be the case for antibody drugs and can also be achieved for small molecules. For example, single-cell imaging has been used to uncover that the immune checkpoint blocker anti-programmed cell death 1 (PD-1) mAb initially binds its intended targets (PD-1 expressed on the surface of T cells) but can then be quickly captured by neighboring macrophages, which limits therapeutic efficacy (Fig. 3B) (25). For PD studies, all reporter systems presented in Table 1 could be deployed to assess a drug's impact on immune components while additional reporters are emerging (12). For example, because IFN- γ is a key factor required for antitumor immunity, IFN- γ -enhanced YFP (eYFP) reporter mice can be used to assess a central readout of successful immunotherapy response (25). PD studies have also shown that radiation therapy can prime tumor-associated macrophages to induce vascular bursts, which enhance drug uptake in the tumor microenvironment (Fig. 3C), and that chemotherapeutics can induce tumor infiltration by myeloid cells, which contribute to chemoresistance (95, 96). Currently, intravital imaging of drug responses focuses mostly on cancer, although existing approaches can be adapted for studies of host defense or autoimmunity.

NEEDS AND EMERGING APPROACHES

Further improvement of intravital single-cell imaging for an improved understanding of immunology will be possible with technological, biological, and computational advances. Technological needs include active and passive methods of motion suppression (24) to image an increasing number of tissues, new chambers and surgical exteriorization methods (9, 19) for imaging in orthotopic organs, photoacoustic microscopy (97–99) for body-wide imaging, infrared imaging and three-photon imaging (97, 100) for deeper imaging (beyond 200 μ m), and implantable microscope optics (101, 102) for imaging over days. Biological needs include new mouse models with fluorescent reporters in multiplex compatible formats for visualizing several immune cell (sub)types simultaneously, new signaling reporters—also in multiplex format—for more detailed understanding of immune cells' molecular activities, as well as labeled antibodies and nano-probes that are validated for intravital microscopy and could also be useful for clinical translation. Computational needs include the development of more efficient analytical software, which could be achieved by adapting deep learning and artificial intelligence solutions (103) and could also be used for whole-organ mapping (104, 105). The combination for single-cell imaging with single-cell RNA sequencing or fluorescence in situ hybridization should also offer deeper integration of physiological data at the cellular and molecular levels (52). Beyond these needs, a number of emerging technologies are on the horizon, including tissue clearing for whole-organ imaging, photoactivatable optogenetic reporters, and photoacoustic microscopy. These methods have considerable potential and applications for immune cell imaging. Tissue clearing methods (such as CLARITY, CUBIC, and C_e3D) reduce light scattering and thus enable deep tissue imaging (106). These methods are still limited to excised and perfused whole organs but nevertheless represent a powerful method for 3D reconstruction of immune cell populations at the whole-organ level (107, 108). Last, photoacoustic microscopy is an innovative high-resolution, high-speed imaging methodology that can provide deeper, larger field-of-view optical contrast, especially when combined

with cell-specific exogenous labeling agents. Although much development has happened at the meso- and macroscopic scales (109), future developments will surely advance the field of immune cell imaging.

REFERENCES AND NOTES

1. F. Balzarotti, Y. Eilers, K. C. Gwosch, A. H. Gynná, V. Westphal, F. D. Stefani, J. Elf, S. W. Hell, Nanometer resolution imaging and tracking of fluorescent molecules with minimal photon fluxes. *Science* **355**, 606–612 (2017).
2. R. Weissleder, M. C. Schwaiger, S. S. Gambhir, H. Hricak, Imaging approaches to optimize molecular therapies. *Sci. Transl. Med.* **8**, 355ps16 (2016).
3. W. R. Zipfel, R. M. Williams, W. W. Webb, Nonlinear magic: Multiphoton microscopy in the biosciences. *Nat. Biotechnol.* **21**, 1369–1377 (2003).
4. M. J. Pittet, R. Weissleder, Intravital imaging. *Cell* **147**, 983–991 (2011).
5. S. I. Ellenbroek, J. van Rheenen, Imaging hallmarks of cancer in living mice. *Nat. Rev. Cancer* **14**, 406–418 (2014).
6. J. Jonkman, C. M. Brown, Any way you slice It—A comparison of confocal microscopy techniques. *J. Biomol. Tech.* **26**, 54–65 (2015).
7. H. D. Hickman, J. R. Bennink, J. W. Yewdell, Caught in the act: Intravital multiphoton microscopy of host-pathogen interactions. *Cell Host Microbe* **5**, 13–31 (2009).
8. S. E. Henrickson, T. R. Mempel, I. B. Mazo, B. Liu, M. N. Artyomov, H. Zheng, A. Peixoto, M. Flynn, B. Senman, T. Junt, H. C. Wong, A. K. Chakraborty, U. H. von Andrian, In vivo imaging of T cell priming. *Sci. Signal.* **1**, pt2 (2008).
9. D. Entenberg, S. Voiculescu, P. Guo, L. Borriello, Y. Wang, G. S. Karagiannis, J. Jones, F. Baccay, M. Oktay, J. Condeelis, A permanent window for the murine lung enables high-resolution imaging of cancer metastasis. *Nat. Methods* **15**, 73–80 (2018).
10. C. Vinegoni, C. Leon Swisher, P. Fumene Feruglio, R. J. Giedt, D. L. Rousso, S. Stapleton, R. Weissleder, Real-time high dynamic range laser scanning microscopy. *Nat. Commun.* **7**, 11077 (2016).
11. J. F. Mohan, R. H. Kohler, J. A. Hill, R. Weissleder, D. Mathis, C. Benoist, Imaging the emergence and natural progression of spontaneous autoimmune diabetes. *Proc. Natl. Acad. Sci. U.S.A.* **114**, E7776–E7785 (2017).
12. M. A. Miller, R. Weissleder, Imaging of anticancer drug action in single cells. *Nat. Rev. Cancer* **17**, 399–414 (2017).
13. M. Alieva, L. Ritsma, R. J. Giedt, R. Weissleder, J. van Rheenen, Imaging windows for long-term intravital imaging. *Intravital* **3**, e29917 (2014).
14. M. Ardigò, M. Agozzino, C. Longo, A. Lallas, V. Di Lernia, A. Fabiano, A. Conti, I. Sperduti, G. Argenziano, E. Berardesca, G. Pellacani, Reflectance confocal microscopy for plaque psoriasis therapeutic follow-up during an anti-TNF- α monoclonal antibody: An observational multicenter study. *J. Eur. Acad. Dermatol. Venereol.* **29**, 2363–2368 (2015).
15. J. Liese, S. H. M. Rooijackers, J. A. G. van Strijp, R. P. Novick, M. L. Dustin, Intravital two-photon microscopy of host-pathogen interactions in a mouse model of *Staphylococcus aureus* skin abscess formation. *Cell. Microbiol.* **15**, 891–909 (2013).
16. D. T. Fisher, J. B. Muhitch, M. Kim, K. C. Doyen, P. N. Bogner, S. S. Evans, J. J. Skitzki, Intraoperative intravital microscopy permits the study of human tumour vessels. *Nat. Commun.* **7**, 10684 (2016).
17. T. T. Murooka, T. R. Mempel, Multiphoton intravital microscopy to study lymphocyte motility in lymph nodes. *Methods Mol. Biol.* **757**, 247–257 (2012).
18. A. Sckell, M. Leunig, Dorsal skinfold chamber preparation in mice: Studying angiogenesis by intravital microscopy. *Methods Mol. Biol.* **1430**, 251–263 (2016).
19. T. Kitamura, J. W. Pollard, M. Vendrell, Optical windows for imaging the metastatic tumour microenvironment in vivo. *Trends Biotechnol.* **35**, 5–8 (2017).
20. J. L. Li, C. C. Goh, J. L. Keeble, J. S. Qin, B. Roediger, R. Jain, Y. Wang, W. K. Chew, W. Wenginger, L. G. Ng, Intravital multiphoton imaging of immune responses in the mouse ear skin. *Nat. Protoc.* **7**, 221–234 (2012).
21. L. Ritsma, E. J. A. Steller, S. I. J. Ellenbroek, O. Kranenburg, I. H. M. Borel Rinkes, J. van Rheenen, Surgical implantation of an abdominal imaging window for intravital microscopy. *Nat. Protoc.* **8**, 583–594 (2013).
22. P. E. Marques, M. M. Antunes, B. A. David, R. V. Pereira, M. M. Teixeira, G. B. Menezes, Imaging liver biology in vivo using conventional confocal microscopy. *Nat. Protoc.* **10**, 258–268 (2015).
23. M. Ferrer, L. Martin-Jaular, M. Calvo, H. A. del Portillo, Intravital microscopy of the spleen: Quantitative analysis of parasite mobility and blood flow. *J. Vis. Exp.* 3609 (2012).
24. C. Vinegoni, A. D. Aguirre, S. Lee, R. Weissleder, Imaging the beating heart in the mouse using intravital microscopy techniques. *Nat. Protoc.* **10**, 1802–1819 (2015).
25. S. P. Arlauckas, C. S. Garriss, R. H. Kohler, M. Kitaoka, M. F. Cuccarese, K. S. Yang, M. A. Miller, J. C. Carlson, G. J. Freeman, R. M. Anthony, R. Weissleder, M. J. Pittet, In vivo imaging reveals a tumor-associated macrophage mediated resistance pathway in anti-PD-1 therapy. *Sci. Transl. Med.* **9**, eaa13604 (2017).
26. Z. Liu, M. Y. Gerner, N. Van Panhuys, A. G. Levine, A. Y. Rudensky, R. N. Germain, Immune homeostasis enforced by co-localized effector and regulatory T cells. *Nature* **528**, 225–230 (2015).
27. J. Fujisaki, J. Wu, A. L. Carlson, L. Silberstein, P. Putheti, R. Larocca, W. Gao, T. I. Saito, C. Lo Celso, H. Tsuyuzaki, T. Sato, D. Côté, M. Sykes, T. B. Strom, D. T. Scadden, C. P. Lin, In vivo imaging of T_{reg} cells providing immune privilege to the haematopoietic stem-cell niche. *Nature* **474**, 216–219 (2011).
28. S. Budhu, D. A. Schaer, Y. Li, R. Toledo-Crow, K. Panageas, X. Yang, H. Zhong, A. N. Houghton, S. C. Silverstein, T. Merghoub, J. D. Wolchok, Blockade of surface-bound TGF- β on regulatory T cells abrogates suppression of effector T cell function in the tumor microenvironment. *Sci. Signal.* **10**, eaak9702 (2017).
29. T. R. Mempel, S. E. Henrickson, U. H. von Andrian, T-cell priming by dendritic cells in lymph nodes occurs in three distinct phases. *Nature* **427**, 154–159 (2004).
30. S. Eickhoff, A. Brewitz, M. Y. Gerner, F. Klauschen, K. Komander, H. Hemmi, N. Garbi, T. Kaisho, R. N. Germain, W. Kastenmüller, Robust anti-viral immunity requires multiple distinct T cell-dendritic cell interactions. *Cell* **162**, 1322–1337 (2015).
31. J. H. Sung, H. Zhang, E. A. Moseman, D. Alvarez, M. Iannacone, S. E. Henrickson, J. C. de la Torre, J. R. Groom, A. D. Luster, U. H. von Andrian, Chemokine guidance of central memory T cells is critical for anti-viral recall responses in lymph nodes. *Cell* **150**, 1249–1263 (2012).
32. J. R. Groom, J. Richmond, T. T. Murooka, E. W. Sorensen, J. H. Sung, K. Bankert, U. H. von Andrian, J. J. Moon, T. R. Mempel, A. D. Luster, CXCR3 chemokine receptor-ligand interactions in the lymph node optimize CD4⁺ T helper 1 cell differentiation. *Immunity* **37**, 1091–1103 (2012).
33. W. Kastenmüller, M. Brandes, Z. Wang, J. Herz, J. G. Egen, R. N. Germain, Peripheral pre-positioning and local CXCL9 chemokine-mediated guidance orchestrate rapid memory CD8⁺ T cell responses in the lymph node. *Immunity* **38**, 502–513 (2013).
34. S. L. Park, A. Zaid, J. L. Hor, S. N. Christo, J. E. Prier, B. Davies, Y. O. Alexandre, J. L. Gregory, T. A. Russell, T. Gebhardt, F. R. Carbone, D. C. Tschärke, W. R. Heath, S. N. Mueller, L. K. Mackay, Local proliferation maintains a stable pool of tissue-resident memory T cells after antiviral recall responses. *Nat. Immunol.* **19**, 183–191 (2018).
35. L. K. Beura, J. S. Mitchell, E. A. Thompson, J. M. Schenkel, J. Mohammed, S. Wijeyesinghe, R. Fonseca, B. J. Burbach, H. D. Hickman, V. Vezys, B. T. Fife, D. Masopust, Intravital mucosal imaging of CD8⁺ resident memory T cells shows tissue-autonomous recall responses that amplify secondary memory. *Nat. Immunol.* **19**, 173–182 (2018).
36. R. S. Friedman, P. Beemiller, C. M. Sorensen, J. Jacobelli, M. F. Krummel, Real-time analysis of T cell receptors in naive cells in vitro and in vivo reveals flexibility in synapse and signaling dynamics. *J. Exp. Med.* **207**, 2733–2749 (2010).
37. F. Marangoni, T. T. Murooka, T. Manzo, E. Y. Kim, E. Carrizosa, N. M. Elpek, T. R. Mempel, The transcription factor NFAT exhibits signal memory during serial T cell interactions with antigen presenting cells. *Immunity* **38**, 237–249 (2013).
38. E. A. Moseman, T. Wu, J. C. de la Torre, P. L. Schwartzberg, D. B. McGavern, Type I interferon suppresses virus-specific B cell responses by modulating CD8⁺ T cell differentiation. *Sci. Immunol.* **1**, eaah3565 (2016).
39. S. Halle, K. A. Keyser, F. R. Stahl, A. Busche, A. Marquardt, X. Zheng, M. Galla, V. Heissmeyer, K. Heller, J. Boelter, K. Wagner, Y. Bischoff, R. Martens, A. Braun, K. Werth, A. Uvarovskii, H. Kempf, M. Meyer-Hermann, R. Arens, M. Kremer, G. Sutter, M. Messerle, R. Förster, In vivo killing capacity of cytotoxic T cells is limited and involves dynamic interactions and T cell cooperativity. *Immunity* **44**, 233–245 (2016).
40. L. G. Guidotti, D. Inverso, L. Sironi, P. Di Lucia, J. Fioravanti, L. Ganzer, A. Fiocchi, M. Vacca, R. Aiolfi, S. Sammiceli, M. Mainetti, T. Cataudella, A. Raimondi, G. Gonzalez-Aseguinolaza, U. Protzer, Z. M. Ruggeri, F. V. Chisari, M. Isogawa, G. Sitia, M. Iannacone, Immunosurveillance of the liver by intravascular effector CD8⁺ T cells. *Cell* **161**, 486–500 (2015).
41. T. R. Mempel, M. J. Pittet, K. Khazaie, W. Wenginger, R. Weissleder, H. von Boehmer, U. H. von Andrian, Regulatory T cells reversibly suppress cytotoxic T cell function independent of effector differentiation. *Immunity* **25**, 129–141 (2006).
42. M. K. Slika, F. Rodriguez, J. L. Whitton, Rapid on/off cycling of cytokine production by virus-specific CD8⁺ T cells. *Nature* **401**, 76–79 (1999).
43. S. S. Cush, G. V. Reynoso, O. Kamenyeva, J. R. Bennink, J. W. Yewdell, H. D. Hickman, Locally produced IL-10 limits cutaneous vaccinia virus spread. *PLOS Pathog.* **12**, e1005493 (2016).
44. R. I. Mazzucchelli, S. Warming, S. M. Lawrence, M. Ishii, M. Abshari, A. V. Washington, L. Feigenbaum, A. C. Warner, D. J. Sims, W. Q. Li, J. A. Hixon, D. H. Gray, B. E. Rich, M. Morrow, M. R. Anver, J. Cherry, D. Naf, L. R. Sternberg, D. W. McVicar, A. G. Farr, R. N. Germain, K. Rogers, N. A. Jenkins, N. G. Copeland, S. K. Durum, Visualization and identification of IL-7 producing cells in reporter mice. *PLOS ONE* **4**, e7637 (2009).

45. T. Junt, E. A. Moseman, M. Iannacone, S. Massberg, P. A. Lang, M. Boes, K. Fink, S. E. Henrickson, D. M. Shayakhmetov, N. C. Di Paolo, N. van Rooijen, T. R. Mempel, S. P. Whelan, U. H. von Andrian, Subcapsular sinus macrophages in lymph nodes clear lymph-borne viruses and present them to antiviral B cells. *Nature* **450**, 110–114 (2007).
46. I. Zaretsky, O. Atrakchi, R. D. Mazor, L. Stoler-Barak, A. Biram, S. W. Feigelson, A. D. Gitlin, B. Engelhardt, Z. Shulman, ICAMs support B cell interactions with T follicular helper cells and promote clonal selection. *J. Exp. Med.* **214**, 3435–3448 (2017).
47. S. Sammicheli, M. Kuka, P. Di Lucia, N. J. de Oya, M. De Giovanni, J. Fioravanti, C. Cristofani, C. G. Maganuco, B. Fallet, L. Ganzer, L. Sironi, M. Mainetti, R. Ostuni, K. Larimore, P. D. Greenberg, J. C. de la Torre, L. G. Guidotti, M. Iannacone, Inflammatory monocytes hinder antiviral B cell responses. *Sci. Immunol.* **1**, eaah6789 (2016).
48. T. I. Arnon, R. M. Horton, I. L. Grigorova, J. G. Cyster, Visualization of splenic marginal zone B cell shuttling and follicular B cell egress. *Nature* **493**, 684–688 (2013).
49. D. Reismann, J. Stefanowski, R. Günther, A. Rakhymzhan, R. Matthys, R. Nützi, S. Zehentmeier, K. Schmidt-Bleek, G. Petkau, H.-D. Chang, S. Naundorf, Y. Winter, F. Melchers, G. Duda, A. E. Hauser, R. A. Niesner, Longitudinal intravital imaging of the femoral bone marrow reveals plasticity within marrow vasculature. *Nat. Commun.* **8**, 2153 (2017).
50. J. H. Kim, J. Podstawka, Y. Lou, L. Li, E. K. S. Lee, M. Divangahi, B. Petri, F. R. Jirik, M. M. Kelly, B. G. Yipp, Aged polymorphonuclear leukocytes cause fibrotic interstitial lung disease in the absence of regulation by B cells. *Nat. Immunol.* **19**, 192–201 (2018).
51. G. D. Victoria, T. A. Schwickert, D. R. Fooksman, A. O. Kamphorst, M. Meyer-Hermann, M. L. Dustin, M. C. Nussenzweig, Germinal center dynamics revealed by multiphoton microscopy using a photoactivatable fluorescent reporter. *Cell* **143**, 592–605 (2010).
52. C. Medaglia, A. Giladi, L. Stoler-Barak, M. De Giovanni, T. M. Salame, A. Biram, E. David, H. Li, M. Iannacone, Z. Shulman, I. Amit, Spatial reconstruction of immune niches by combining photoactivatable reporters and scRNA-seq. *Science* **358**, 1622–1626 (2017).
53. M. Y. Gerner, P. Torabi-Parizi, R. N. Germain, Strategically localized dendritic cells promote rapid T cell responses to lymph-borne particulate antigens. *Immunity* **42**, 172–185 (2015).
54. A. Brewitz, S. Eickhoff, S. Dähling, T. Quast, S. Bedoui, R. A. Kroczyk, C. Kurts, N. Garbi, W. Barchet, M. Iannacone, F. Klauschen, W. Kolanus, T. Kaisho, M. Colonna, R. N. Germain, W. Kastenmüller, CD8⁺ T cells orchestrate pDC-XCR1⁺ dendritic cell spatial and functional cooperativity to optimize priming. *Immunity* **46**, 205–219 (2017).
55. M. Kitano, C. Yamazaki, A. Takumi, T. Ikeno, H. Hemmi, N. Takahashi, K. Shimizu, S. E. Fraser, K. Hoshino, T. Kaisho, T. Okada, Imaging of the cross-presenting dendritic cell subsets in the skin-draining lymph node. *Proc. Natl. Acad. Sci. U.S.A.* **113**, 1044–1049 (2016).
56. J. L. Hor, P. G. Whitney, A. Zaid, A. G. Brooks, W. R. Heath, S. N. Mueller, Spatiotemporally distinct interactions with dendritic cell subsets facilitates CD4⁺ and CD8⁺ T cell activation to localized viral infection. *Immunity* **43**, 554–565 (2015).
57. F. Castellino, A. Y. Huang, G. Altan-Bonnet, S. Stoll, C. Scheinecker, R. N. Germain, Chemokines enhance immunity by guiding naive CD8⁺ T cells to sites of CD4⁺ T cell–dendritic cell interaction. *Nature* **440**, 890–895 (2006).
58. P. Sagoo, Z. Garcia, B. Breart, F. Lemaître, D. Michonneau, M. L. Albert, Y. Levy, P. Bousso, In vivo imaging of inflammasome activation reveals a subcapsular macrophage burst response that mobilizes innate and adaptive immunity. *Nat. Med.* **22**, 64–71 (2016).
59. G. S. Karagiannis, J. M. Pastoriza, Y. Wang, A. S. Harney, D. Entenberg, J. Pignatelli, V. P. Sharma, E. A. Xue, E. Cheng, T. M. D'Alfonso, J. G. Jones, J. Anampa, T. E. Rohan, J. A. Sparano, J. S. Condeelis, M. H. Oktay, Neoadjuvant chemotherapy induces breast cancer metastasis through a TMEM-mediated mechanism. *Sci. Transl. Med.* **9**, eaan0026 (2017).
60. J. B. Wyckoff, Y. Wang, E. Y. Lin, J. F. Li, S. Goswami, E. R. Stanley, J. E. Segall, J. W. Pollard, J. Condeelis, Direct visualization of macrophage-assisted tumor cell intravasation in mammary tumors. *Cancer Res.* **67**, 2649–2656 (2007).
61. J. Wang, P. Kubes, A reservoir of mature cavity macrophages that can rapidly invade visceral organs to affect tissue repair. *Cell* **165**, 668–678 (2016).
62. M. B. Headley, A. Bins, A. Nip, E. W. Roberts, M. R. Looney, A. Gerard, M. F. Krummel, Visualization of immediate immune responses to pioneer metastatic cells in the lung. *Nature* **531**, 513–517 (2016).
63. M. Finsterbusch, P. Hall, A. Li, S. Devi, C. L. V. Westhorpe, A. R. Kitching, M. J. Hickey, Patrolling monocytes promote intravascular neutrophil activation and glomerular injury in the acutely inflamed glomerulus. *Proc. Natl. Acad. Sci. U.S.A.* **113**, E5172–E5181 (2016).
64. D. Nayak, K. R. Johnson, S. Heydari, T. L. Roth, B. H. Zinselmeyer, D. B. McGavern, Type I interferon programs innate myeloid dynamics and gene expression in the virally infected nervous system. *PLOS Pathog.* **9**, e1003395 (2013).
65. R. Weissleder, M. Nahrendorf, M. J. Pittet, Imaging macrophages with nanoparticles. *Nat. Mater.* **13**, 125–138 (2014).
66. D. Davalos, J. Grutzendler, G. Yang, J. V. Kim, Y. Zuo, S. Jung, D. R. Littman, M. L. Dustin, W.-B. Gan, ATP mediates rapid microglial response to local brain injury in vivo. *Nat. Neurosci.* **8**, 752–758 (2005).
67. Z. Zeng, B. G. Surewaard, C. H. Wong, J. A. Geoghegan, C. N. Jenne, P. Kubes, CRLG functions as a macrophage pattern recognition receptor to directly bind and capture blood-borne gram-positive bacteria. *Cell Host Microbe* **20**, 99–106 (2016).
68. D. H. Madsen, H. J. Jürgensen, M. S. Siersbæk, D. E. Kuczek, L. Grey Cloud, S. Liu, N. Behrendt, L. Grøntved, R. Weigert, T. H. Bugge, Tumor-associated macrophages derived from circulating inflammatory monocytes degrade collagen through cellular uptake. *Cell Rep.* **21**, 3662–3671 (2017).
69. A. Nimmerjahn, F. Kirchhoff, F. Helmchen, Resting microglial cells are highly dynamic surveillants of brain parenchyma in vivo. *Science* **308**, 1314–1318 (2005).
70. M. Ruh-Johnson, A. N. Shah, J. A. Stonick, K. R. Poudel, J. Kargl, G. H. Yang, J. di Martino, R. E. Hernandez, C. E. Gast, L. R. Zour, S. Antoku, A. M. Houghton, J. J. Bravo-Cordero, M. H. Wong, J. Condeelis, C. B. Moens, Macrophage-dependent cytoplasmic transfer during melanoma invasion in vivo. *Dev. Cell* **43**, 549–562.e6 (2017).
71. M. A. Miller, R. Chandra, M. F. Cuccarese, C. Pfirschke, C. Engblom, S. Stapleton, U. Adhikary, R. H. Kohler, J. F. Mohan, M. J. Pittet, R. Weissleder, Radiation therapy primes tumors for nanotherapeutic delivery via macrophage-mediated vascular bursts. *Sci. Transl. Med.* **9**, eaal0225 (2017).
72. D. K. Fogg, C. Sibon, C. Miled, S. Jung, P. Aucouturier, D. R. Littman, A. Cumano, F. Geissmann, A clonogenic bone marrow progenitor specific for macrophages and dendritic cells. *Science* **311**, 83–87 (2006).
73. F. K. Swirski, M. Nahrendorf, M. Etzrodt, M. Wildgruber, V. Cortez-Retamozo, P. Panizzi, J.-L. Figueiredo, R. H. Kohler, A. Chudnovskiy, P. Waterman, E. Aikawa, T. R. Mempel, P. Libby, R. Weissleder, M. J. Pittet, Identification of splenic reservoir monocytes and their deployment to inflammatory sites. *Science* **325**, 612–616 (2009).
74. C. Stremmel, R. Schuchert, F. Wagner, R. Thaler, T. Weinberger, R. Pick, E. Mass, H. C. Ishikawa-Ankerhold, A. Margraf, S. Hutter, R. Vagnozzi, S. Klapproth, J. Frampton, S. Yona, C. Scheiermann, J. D. Molkenin, U. Jeschke, M. Moser, M. Sperandio, S. Massberg, F. Geissmann, C. Schulz, Yolk sac macrophage progenitors traffic to the embryo during defined stages of development. *Nat. Commun.* **9**, 75 (2018).
75. J. Wang, M. Hossain, A. Thanabalasuriar, M. Gunzer, C. Meininger, P. Kubes, Visualizing the function and fate of neutrophils in sterile injury and repair. *Science* **358**, 111–116 (2017).
76. B. G. Yipp, J. H. Kim, R. Lima, L. D. Zbytniuk, B. Petri, N. Swanlund, M. Ho, V. G. Szeto, T. Tak, L. Koenderman, P. Pickers, A. T. J. Tool, T. W. Kuijpers, T. K. van den Berg, M. R. Looney, M. F. Krummel, P. Kubes, The lung is a host defense niche for immediate neutrophil-mediated vascular protection. *Sci. Immunol.* **2**, eaam8929 (2017).
77. T. Lämmermann, P. V. Afonso, B. R. Angermann, J. M. Wang, W. Kastenmüller, C. A. Parent, R. N. Germain, Neutrophil swarms require LTB4 and integrins at sites of cell death in vivo. *Nature* **498**, 371–375 (2013).
78. J. F. Deniset, B. G. Surewaard, W.-Y. Lee, P. Kubes, Splenic Ly6G^{high} mature and Ly6G^{int} immature neutrophils contribute to eradication of *S. pneumoniae*. *J. Exp. Med.* **214**, 1333–1350 (2017).
79. Y. Miyabe, C. Miyabe, T. T. Murooka, E. Y. Kim, G. A. Newton, N. D. Kim, B. Haribabu, F. W. Lusinskas, T. R. Mempel, A. D. Luster, Complement C5a receptor is the key initiator of neutrophil adhesion igniting immune complex-induced arthritis. *Sci. Immunol.* **2**, eaaj2195 (2017).
80. K. Lim, Y.-M. Hyun, K. Lambert-Emo, T. Capece, S. Bae, R. Miller, D. J. Topham, M. Kim, Neutrophil trails guide influenza-specific CD8⁺ T cells in the airways. *Science* **349**, aaa4352 (2015).
81. J. Park, R. W. Wysocki, Z. Amoozgar, L. Maiorino, M. R. Fein, J. Jorns, A. F. Schott, Y. Kinugasa-Katayama, Y. Lee, N. H. Won, E. S. Nakasone, S. A. Hearn, V. Küttner, J. Qiu, A. S. Almeida, N. Perurena, K. Kessenbrock, M. S. Goldberg, M. Egeblad, Cancer cells induce metastasis-supporting neutrophil extracellular DNA traps. *Sci. Transl. Med.* **8**, 361ra138 (2016).
82. E. Kolaczowska, C. N. Jenne, B. G. J. Surewaard, A. Thanabalasuriar, W.-Y. Lee, M.-J. Sanz, K. Mowen, G. Opendakker, P. Kubes, Molecular mechanisms of NET formation and degradation revealed by intravital imaging in the liver vasculature. *Nat. Commun.* **6**, 6673 (2015).
83. I. B. Mazo, J.-C. Gutierrez-Ramos, P. S. Frenette, R. O. Hynes, D. D. Wagner, U. H. von Andrian, Hematopoietic progenitor cell rolling in bone marrow microvessels: Parallel contributions by endothelial selectins and vascular cell adhesion molecule 1. *J. Exp. Med.* **188**, 465–474 (1998).
84. V. Cortez-Retamozo, M. Etzrodt, A. Newton, P. J. Rauch, A. Chudnovskiy, C. Berger, R. J. H. Ryan, Y. Iwamoto, B. Marinelli, R. Gorbato, R. Forghani, T. I. Novobrantseva,

- V. Kotliansky, J. L. Figueiredo, J. W. Chen, D. G. Anderson, M. Nahrendorf, F. K. Swirski, R. Weissleder, M. J. Pittet, Origins of tumor-associated macrophages and neutrophils. *Proc. Natl. Acad. Sci. U.S.A.* **109**, 2491–2496 (2012).
85. C. N. Jenne, C. H. Wong, F. J. Zemp, B. McDonald, M. M. Rahman, P. A. Forsyth, G. McFadden, P. Kubers, Neutrophils recruited to sites of infection protect from virus challenge by releasing neutrophil extracellular traps. *Cell Host Microbe* **13**, 169–180 (2013).
86. C. H. Y. Wong, C. N. Jenne, B. Petri, N. L. Chrobok, P. Kubers, Nucleation of platelets with bloodborne pathogens on Kupffer cell precedes other innate immunity and contributes to bacterial clearance. *Nat. Immunol.* **14**, 785–792 (2013).
87. F. Gaertner, Z. Ahmad, G. Rosenberger, S. Fan, L. Nicolai, B. Busch, G. Yavuz, M. Luckner, H. Ishikawa-Ankerhold, R. Hennel, A. Benechet, M. Lorenz, S. Chandraratne, I. Schubert, S. Helmer, B. Striednig, K. Stark, M. Janko, R. T. Böttcher, A. Verschoor, C. Leon, C. Gachet, T. Gudermann, Y. Mederos, M. Schnitzler, Z. Pincus, M. Iannaccone, R. Haas, G. Wanner, K. Lauber, M. Sixt, S. Massberg, Migrating platelets are mechano-scavengers that collect and bundle bacteria. *Cell* **171**, 1368–1382.e23 (2017).
88. E. Lefrançois, G. Ortiz-Muñoz, A. Caudrillier, B. Mallavia, F. Liu, D. M. Sayah, E. E. Thornton, M. B. Headley, T. David, S. R. Coughlin, M. F. Krummel, A. D. Leavitt, E. Passegué, M. R. Looney, The lung is a site of platelet biogenesis and a reservoir for hematopoietic progenitors. *Nature* **544**, 105–109 (2017).
89. P. X. Liew, W. Y. Lee, P. Kubers, iNKT cells orchestrate a switch from inflammation to resolution of sterile liver injury. *Immunity* **47**, 752–765.e5 (2017).
90. C. H. Y. Wong, C. N. Jenne, W.-Y. Lee, C. Léger, P. Kubers, Functional innervation of hepatic iNKT cells is immunosuppressive following stroke. *Science* **334**, 101–105 (2011).
91. B. Roediger, R. Kyle, K. H. Yip, N. Sumaria, T. V. Guy, B. S. Kim, A. J. Mitchell, S. S. Tay, R. Jain, E. Forbes-Blom, X. Chen, P. L. Tong, H. A. Bolton, D. Artis, W. E. Paul, B. Fazekas de St Groth, M. A. Grimbaldston, G. Le Gros, W. Weninger, Cutaneous immuno-surveillance and regulation of inflammation by group 2 innate lymphoid cells. *Nat. Immunol.* **14**, 564–573 (2013).
92. J. Deguine, B. Breart, F. Lemaître, J. P. Di Santo, P. Bousso, Intravital imaging reveals distinct dynamics for natural killer and CD8⁺ T cells during tumor regression. *Immunity* **33**, 632–644 (2010).
93. M. Gaya, P. Barral, M. Burbage, S. Aggarwal, B. Montaner, A. Warren Navia, M. Aid, C. Tsui, P. Maldonado, U. Nair, K. Ghneim, P. G. Fallon, R.-P. Sekaly, D. H. Barouch, A. K. Shalek, A. Bruckbauer, J. Strid, F. D. Batista, Initiation of antiviral B cell immunity relies on innate signals from spatially positioned NKT cells. *Cell* **172**, 517–533.e20 (2018).
94. M. A. Miller, Y.-R. Zheng, S. Gadde, C. Pfirschke, H. Zope, C. Engblom, R. H. Kohler, Y. Iwamoto, K. S. Yang, B. Askevold, N. Kolisshetti, M. Pittet, S. J. Lippard, O. C. Farokhzad, R. Weissleder, Tumour-associated macrophages act as a slow-release reservoir of nano-therapeutic Pt(IV) pro-drug. *Nat. Commun.* **6**, 8692 (2015).
95. E. S. Nakasone, H. A. Askautrud, T. Kees, J.-H. Park, V. Plaks, A. J. Ewald, M. Fein, M. G. Rasch, Y.-X. Tan, J. Qiu, J. Park, P. Sinha, M. J. Bissell, E. Frengen, Z. Werb, M. Egeblad, Imaging tumor-stroma interactions during chemotherapy reveals contributions of the microenvironment to resistance. *Cancer Cell* **21**, 488–503 (2012).
96. C. Engblom, C. Pfirschke, M. J. Pittet, The role of myeloid cells in cancer therapies. *Nat. Rev. Cancer* **16**, 447–462 (2016).
97. G. Hong, S. Diao, J. Chang, A. L. Antaris, C. Chen, B. Zhang, S. Zhao, D. N. Atochin, P. L. Huang, K. I. Andreasson, C. J. Kuo, H. Dai, Through-skull fluorescence imaging of the brain in a new near-infrared window. *Nat. Photonics* **8**, 723–730 (2014).
98. L. V. Wang, S. Hu, Photoacoustic tomography: In vivo imaging from organelles to organs. *Science* **335**, 1458–1462 (2012).
99. J. Yao, L. Wang, J.-M. Yang, K. I. Maslov, T. T. W. Wong, L. Li, C.-H. Huang, J. Zou, L. V. Wang, High-speed label-free functional photoacoustic microscopy of mouse brain in action. *Nat. Methods* **12**, 407–410 (2015).
100. C. J. Rowlands, D. Park, O. T. Bruns, K. D. Piatkevich, D. Fukumura, R. K. Jain, M. G. Bawendi, E. S. Boyden, P. T. C. So, Wide-field three-photon excitation in biological samples. *Light Sci. Appl.* **6**, e16255 (2017).
101. E. J. O. Hamel, B. F. Grewe, J. G. Parker, M. J. Schnitzer, Cellular level brain imaging in behaving mammals: An engineering approach. *Neuron* **86**, 140–159 (2015).
102. T. H. Kim, Y. Zhang, J. Lecoq, J. C. Jung, J. Li, H. Zeng, C. M. Niell, M. J. Schnitzer, Long-term optical access to an estimated one million neurons in the live mouse cortex. *Cell Rep.* **17**, 3385–3394 (2016).
103. T. Ching, D. S. Himmelstein, B. K. Beaulieu-Jones, A. A. Kalinin, B. T. Do, G. P. Way, E. Ferrero, P.-M. Agapow, M. Zietz, M. M. Hoffman, W. Xie, G. L. Rosen, B. J. Lengerich, J. Israeli, J. Lanchantin, S. Woloszynek, A. E. Carpenter, A. Shrikumar, J. Xu, E. M. Cofer, C. A. Lavender, S. C. Turaga, A. M. Alexandari, Z. Lu, D. J. Harris, D. DeCaprio, Y. Qi, A. Kundaje, Y. Peng, L. K. Wiley, M. H. S. Segler, S. M. Boca, S. J. Swamidass, A. Huang, A. Gitter, C. S. Greene, Opportunities and obstacles for deep learning in biology and medicine. *J. R. Soc. Interface* **15**, (2018).
104. M. N. Economo, N. G. Clack, L. D. Lavis, C. R. Gerfen, K. Svoboda, E. W. Myers, J. Chandrashekar, A platform for brain-wide imaging and reconstruction of individual neurons. *eLife* **5**, e10566 (2016).
105. N. Tanaka, S. Kanatani, R. Tomer, C. Sahlgren, P. Kronqvist, D. Kaczynska, L. Louhivuori, L. Kis, C. Lindh, P. Mitura, A. Stepulak, S. Corvigno, J. Hartman, P. Micke, A. Mezheyeuski, C. Strell, J. W. Carlson, C. Fernandez Moro, H. Dahlstrand, A. Östman, K. Matsumoto, P. Wiklund, M. Oya, A. Miyakawa, K. Deisseroth, P. Uhlen, Whole-tissue biopsy phenotyping of three-dimensional tumours reveals patterns of cancer heterogeneity. *Nat. Biomed. Eng.* **1**, 796–806 (2017).
106. D. S. Richardson, J. W. Lichtman, Clarifying tissue clearing. *Cell* **162**, 246–257 (2015).
107. M. F. Cuccarese, J. M. Dubach, C. Pfirschke, C. Engblom, C. Garriss, M. A. Miller, M. J. Pittet, R. Weissleder, Heterogeneity of macrophage infiltration and therapeutic response in lung carcinoma revealed by 3D organ imaging. *Nat. Commun.* **8**, 14293 (2017).
108. W. Li, R. N. Germain, M. Y. Gerner, Multiplex, quantitative cellular analysis in large tissue volumes with clearing-enhanced 3D microscopy (Ca3D). *Proc. Natl. Acad. Sci. U.S.A.* **114**, E7321–E7330 (2017).
109. J. Ripoll, B. Koberstein-Schwarz, V. Ntziachristos, Unleashing optics and optoacoustics for developmental biology. *Trends Biotechnol.* **33**, 679–691 (2015).
110. A. E. Moran, K. L. Holzapfel, Y. Xing, N. R. Cunningham, J. S. Maltzman, J. Punt, K. A. Hogquist, T cell receptor signal strength in T_{reg} and iNKT cell development demonstrated by a novel fluorescent reporter mouse. *J. Exp. Med.* **208**, 1279–1289 (2011).
111. P. Mouchacca, A.-M. Schmitt-Verhulst, C. Boyer, Visualization of cytolytic T cell differentiation and granule exocytosis with T cells from mice expressing active fluorescent granzyme B. *PLOS ONE* **8**, e67239 (2013).
112. J. Zhu, D. Jankovic, A. J. Oler, G. Wei, S. Sharma, G. Hu, L. Guo, R. Yagi, H. Yamane, G. P. Puskosy, L. Feigenbaum, K. Zhao, W. E. Paul, The transcription factor T-bet is induced by multiple pathways and prevents an endogenous T helper-2 program during T helper-1 responses. *Immunity* **37**, 660–673 (2012).
113. K. Singbartl, J. Thatte, M. L. Smith, K. Wethmar, K. Day, K. Ley, A CD2-green fluorescence protein-transgenic mouse reveals very late antigen-4 dependent CD8⁺ lymphocyte rolling in inflamed venules. *J. Immunol.* **166**, 7520–7526 (2001).
114. A. L. Croxford, F. C. Kurschus, A. Waisman, Cutting edge: An IL-17-Cre^{EYFP} reporter mouse allows fate mapping of Th17 cells. *J. Immunol.* **182**, 1237–1241 (2009).
115. M. Mohrs, K. Shinkai, K. Mohrs, R. M. Locksley, Analysis of type 2 immunity in vivo with a bicistronic IL-4 reporter. *Immunity* **15**, 303–311 (2001).
116. K. Lüthje, A. Kallies, Y. Shimohakamada, G. T. Belz, A. Light, D. M. Tarlinton, S. L. Nutt, The development and fate of follicular helper T cells defined by an IL-21 reporter mouse. *Nat. Immunol.* **13**, 491–498 (2012).
117. H. Qi, J. G. Egen, A. Y. C. Huang, R. N. Germain, Extrafollicular activation of lymph node B cells by antigen-bearing dendritic cells. *Science* **312**, 1672–1676 (2006).
118. M. Kitano, S. Moriyama, Y. Ando, M. Hikida, Y. Mori, T. Kurosaki, T. Okada, Bcl6 protein expression shapes pre-germinal center B cell dynamics and follicular helper T cell heterogeneity. *Immunity* **34**, 961–972 (2011).
119. D. R. Fooksman, T. A. Schwickert, G. D. Victora, M. L. Dustin, M. C. Nussenzweig, D. Skokos, Development and migration of pre-plasma cells in the mouse lymph node. *Immunity* **33**, 118–127 (2010).
120. E. E. Crouch, Z. Li, M. Takizawa, S. Fichtner-Feigl, P. Gourzi, C. Montano, L. Feigenbaum, P. Wilson, S. Janz, F. N. Papavasiliou, R. Casellas, Regulation of AID expression in the immune response. *J. Exp. Med.* **204**, 1145–1156 (2007).
121. J. J. Engelhardt, B. Boldajipour, P. Beemiller, P. Pandurangi, C. Sorensen, Z. Werb, M. Egeblad, M. F. Krummel, Marginating dendritic cells of the tumor microenvironment cross-present tumor antigens and stably engage tumor-specific T cells. *Cancer Cell* **21**, 402–417 (2012).
122. A. T. Satpathy, W. KC, J. C. Albring, B. T. Edelson, N. M. Kretzer, D. Bhattacharya, T. L. Murphy, K. M. Murphy, *Zbtb46* expression distinguishes classical dendritic cells and their committed progenitors from other immune lineages. *J. Exp. Med.* **209**, 1135–1152 (2012).
123. C. Auffray, D. Fogg, M. Garfa, G. Elaine, O. Join-Lambert, S. Kayal, S. Sarnacki, A. Cumano, G. Lauvau, F. Geissmann, Monitoring of blood vessels and tissues by a population of monocytes with patrolling behavior. *Science* **317**, 666–670 (2007).
124. K. A. Sauter, C. Pridans, A. Sehgal, C. C. Bain, C. Scott, L. Moffat, R. Rojo, B. M. Stutchfield, C. L. Davies, D. S. Donaldson, K. Renault, B. W. McCall, A. M. Mowat, A. Serrels, M. C. Frame, N. A. Mabbott, D. A. Hume, The macblue binary transgene (csf1-gal4VP16/UAS-EYFP) provides a novel marker for visualisation of subsets of monocytes, macrophages and dendritic cells and responsiveness to CSF1 administration. *PLOS ONE* **9**, e105429 (2014).
125. E. E. Gray, S. Friend, K. Suzuki, T. G. Phan, J. G. Cyster, Subcapsular sinus macrophage fragmentation and CD169⁺ bleb acquisition by closely associated IL-17-committed innate-like lymphocytes. *PLOS ONE* **7**, e38258 (2012).
126. J. Cools-Lartigue, J. Spicer, B. McDonald, S. Gowing, S. Chow, B. Giannias, F. Bourdeau, P. Kubers, L. Ferri, Neutrophil extracellular traps sequester circulating tumor cells and promote metastasis. *J. Clin. Invest.* **123**, 3446–3458 (2013).

127. A. Jayagopal, P. K. Russ, F. R. Haselton, Surface engineering of quantum dots for in vivo vascular imaging. *Bioconjug. Chem.* **18**, 1424–1233 (2007).
128. R. Darbousset, G. M. Thomas, S. Mezouar, C. Frère, R. Bonier, N. Mackman, T. Renné, F. Dignat-George, C. Dubois, L. Panicot-Dubois, Tissue factor–positive neutrophils bind to injured endothelial wall and initiate thrombus formation. *Blood* **120**, 2133–2143 (2012).

Acknowledgments: We apologize to the authors whose work we could not cite because of space constraints. **Funding:** The work of M.J.P. is supported by NIH grants R01-AI084880, R01-CA206890, R01-CA218579, and R01-AI123349 and the Samana Cay Massachusetts General Hospital Research Scholar Fund. C.S.G. and S.P.A. are supported by NIH grants F31-CA196035

and T32-CA79443, respectively. The work of R.W. is supported by NIH grants R33-CA202064, R01-CA206890, and U01CA206997.

Submitted 8 March 2018
Accepted 24 July 2018
Published 7 September 2018
10.1126/sciimmunol.aaq0491

Citation: M. J. Pittet, C. S. Garris, S. P. Arlauckas, R. Weissleder, Recording the wild lives of immune cells. *Sci. Immunol.* **3**, eaaq0491 (2018).

Recording the wild lives of immune cells

Mikael J. Pittet, Christopher S. Garris, Sean P. Arlauckas and Ralph Weissleder

Sci. Immunol. **3**, eaaq0491.
DOI: 10.1126/sciimmunol.aaq0491

ARTICLE TOOLS

<http://immunology.sciencemag.org/content/3/27/eaaq0491>

REFERENCES

This article cites 126 articles, 38 of which you can access for free
<http://immunology.sciencemag.org/content/3/27/eaaq0491#BIBL>

Use of this article is subject to the [Terms of Service](#)

Science Immunology (ISSN 2470-9468) is published by the American Association for the Advancement of Science, 1200 New York Avenue NW, Washington, DC 20005. 2017 © The Authors, some rights reserved; exclusive licensee American Association for the Advancement of Science. No claim to original U.S. Government Works. The title *Science Immunology* is a registered trademark of AAAS.